ISSN 1807-1929
Revista Brasileira de Engenharia Agrícola e Ambiental
Brazilian Journal of Agricultural and Environmental Engineering
v.29, n.2, e281773, 2025
Campina Grande, PB – http://www.agriambi.com.br – http://www.scielo.br/rbeaa

DOI: http://dx.doi.org/10.1590/1807-1929/agriambi.v29n2e281773 ORIGINAL ARTICLE

Optimal structure selection of emitter flow path in drip irrigation system with inferior water resources[1]

Seleção ideal da estrutura do caminho do fluxo do emissor em sistema de irrigação por gotejamento com recursos hídricos inferiores

Ji Feng[2*], Haisheng Liu[3], Yanzheng Liu[2], Haosu Sun[4], Changjian Ma[5], Puchen Shi[6], Weinan Wang[7], Song Xue[8] & Jiangli Wen[2]

[1] Research developed at Beijing Vocational College of Agriculture/Department of Water Resources and Architectural Engineering, Beijing, China
[2] Beijing Vocational College of Agriculture/Department of Water Resources and Architectural Engineering, Beijing, China
[3] Zhejiang Tongji Vocational College of Science and Technology, Hangzho, China
[4] Daning Management Office of Beijing South-to-North Water Transfer Project, Beijing, China
[5] Shandong Academy of Agricultural Sciences, Jinan, China
[6] Beijing Urban Rivers and Lakes Management Office, Beijing, China
[7] Beijing Changping District Drainage Service Center, Beijing, China
[8] Shanxi Weihe River Ecological Zone Protection Center, Xian, China

HIGHLIGHTS:

Optimal structure of emitter flow path is selected using inferior water sources.
Hydraulic performance and anti-clogging ability of emitter are studied comprehensively.
Flow characteristics within composite clogging emitter are visualized.

ABSTRACT: The fundamental solution to the problem of emitter clogging is to explore the optimal structure design of emitter and improve its anti-clogging ability. The research objective was to select the optimal structural form of the emitter flow path in drip irrigation systems using inferior water sources, which can provide theoretical support for improving the anti-clogging ability of the emitter itself and designing new emitter products. The selection of the flow path structure of the emitter has not been conducted on the basis of determining the appropriate simulation model with the condition of complex water quality. Therefore, the appropriate internal fluid movement model of the emitter was determined, the hydraulic performance and anti-clogging performance of the five nationally and internationally representative flow path structures were comprehensively evaluated, and finally the optimal structure of the emitter flow path was determined. The research results indicated that RNG k - ε model was the most suitable to simulate the flow field in the emitter by comprehensive analysis of the gap between simulated values and the measured values, the calculation accuracy and computational efficiency. The fractal flow path was relatively optimal for hydraulic performance and for anti-clogging performance. This study can provide theoretical support for improving the anti-clogging ability of the emitter itself and the design of the new emitter product.

Key words: hydraulic performance, anti-clogging performance, numerical simulation

RESUMO: A solução fundamental para o problema do entupimento do emissor é explorar o projeto ideal da estrutura do emissor e melhorar sua capacidade anti-entupimento. O objetivo da pesquisa foi selecionar a forma estrutural ideal do caminho de fluxo do emissor em sistemas de irrigação por gotejamento utilizando fontes de água de qualidade inferior, proporcionando suporte teórico para melhorar a capacidade anti-obstrução do próprio emissor e para o projeto de novos produtos de emissores. A seleção da estrutura do caminho do fluxo do emissor não tem sido conduzida com base na determinação do modelo de simulação apropriado com a condição complexa de qualidade da água. Para tanto, determinou-se o modelo de movimento interno do fluido adequado do emissor, e avaliou-se de forma abrangente o desempenho hidráulico e o desempenho anti-entupimento das cinco estruturas representativas da trajetória de fluxo no país e no exterior, e finalmente determinou-se a estrutura ótima da trajetória de fluxo do emissor. Os resultados da pesquisa indicaram que o modelo RNG k-ε foi o mais adequado para simular a área do fluxo no emissor por meio da análise abrangente da lacuna entre os valores simulados e os valores medidos, da precisão do cálculo e da eficiência computacional. A trajetória de fluxo fractal foi relativamente ótima para o desempenho hidráulico e para o desempenho anti-entupimento. Este estudo pode fornecer suporte teórico para melhorar a própria habilidade anti-obstrução do emissor e o projeto de novo produto de emissor.

Palavras-chave: desempenho hidráulico, desempenho anti-entupimento, simulação numérica

• Ref. 281773 – Received 26 Dec, 2023
* Corresponding author - E-mail: fengji661779@163.com
• Accepted 28 Jul, 2024 • Published 28 Aug, 2024
Editors: Ítalo Herbet Lucena Cavalcante & Carlos Alberto Vieira de Azevedo

Introduction

Drip irrigation technology has become one of the most widely used modern high-efficiency water-saving irrigation technologies due to its precision and controllability (Tayel et al., 2013; Li et al., 2019a; Feng et al., 2019). Emitter clogging has become an international problem in the field of drip irrigation (Li et al., 2012; Chai, 2016; Song et al., 2020). In addition, low quality water sources are usually used as water sources for drip irrigation because water pollution is becoming more and more serious with the global shortage of water resources and the acceleration of industrialization (Xue, 2016; Li et al., 2019b).

In these water sources，particulate matter mainly exists in the form of microbial flocculation with a layer of biofilm attached to the surface (Li et al., 2015; Liu et al., 2016). This emitter clogging is compound clogging under the condition of the coupled action of multiple factors, which make the problem of solving the emitter clogging more difficult. A large number of scholars have worked to reduce emitter clogging through multiple approaches (Elbana et al., 2012; Han et al., 2018; Jiao et al., 2020; Liu et al., 2021a; Liu et al., 2021b; Zhou et al., 2021). However, this problem still has not been effectively solved. The core and key to solve the problem is to improve the anti-clogging ability of the emitter (Nakayama & Bucks, 1991; Han et al., 2019).

Optimizing the structure design is an effective way to improve the anti-clogging ability of the emitter. In the structure design process of the emitter, the structure style of the emitter path is one of the key aspects that effect its hydraulic performance and anti-clogging performance (Markku et al., 2006; Feng et al., 2018; Muhammad et al., 2021). Therefore, the objective of this research was to determine the appropriate internal fluid movement model of the emitter, to comprehensively evaluate the hydraulic performance and the anti-clogging performance of the five nationally and internationally representative flow path structures, and finally to determine the optimal structure of the emitter flow path.

The research objective was to select the optimal structural form of the emitter flow path in drip irrigation systems using inferior water sources, which can provide theoretical support for improving the anti-clogging ability of the emitter itself and the design of new emitter products.

Material and Methods

In this study, emitters from representative domestic and foreign manufacturers were investigated and five types of flow paths were determined to simulate the flow characteristics of water. They were respectively trapezoid flow path (with the discharge of 2.2 L h^{-1} from Longda in Hebei, China), saw-tooth flow path (with the discharge of 1.38 L h^{-1} from Netafim in Israel), rectangle flow path (with the discharge of 3.0 L h^{-1} from Yameite in Gansu, China), triangle flow path (with the discharge of 2.0 L h^{-1} from Yameite in Gansu, China), and fractal flow path designed by the team of this research (with the discharge of 2.0 L h^{-1}). Their structures are shown in Table 1.

The structure of emitter flow path mainly includes three parts: inlet, outlet and flow path (Feng et al., 2018). In order to make the numerical calculation result closer to the actual situation, the construction of the calculation domain included all the main parts of the flow path. The GAMBIT (The name of a module used for grid partitioning in software) module of ANSYS (The name of large universal finite element analysis (FEA) software developed by ANSYS in the United States) which was adopted to draw the calculation domain through which the water flow passes, and calculation domain of flow path is shown in Figure 1A.

In this study, the hexahedral mesh was adopted to grid the calculation domain by ANSYS ICEM software, and encrypted the near-wall surface, corner and tooth tip to more accurately

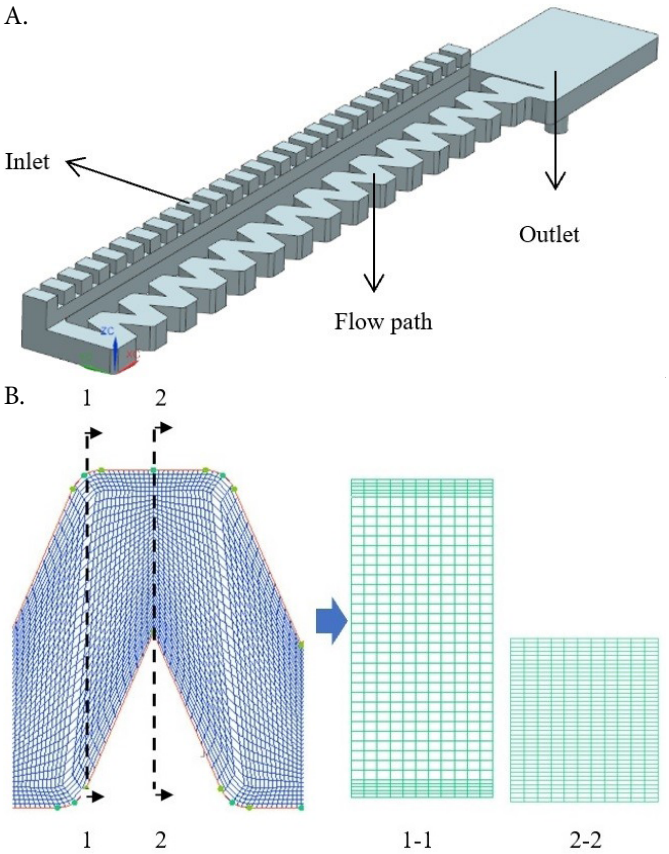

1-1 – Flow path in a vertical section of the grid; 2-2 – Flow path in another vertical section of the grid

Figure 1. The calculation domain (A) and mesh generating (B) of emitter flow path

Table 1. Illustrations of the structural unit of flow path of different emitters

Trapezoid flow path	Saw-tooth flow path	Rectangle flow path	Triangle flow path	Fractal flow path
	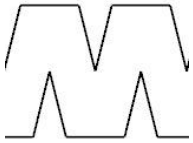	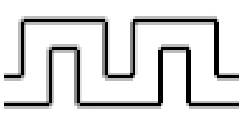		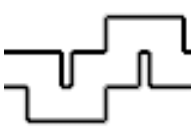

simulate the flow characteristics in the dramatic change region. The density of the grid influences calculation accuracy and calculation efficiency (Feng et al., 2018), so the number of grids should be reduced to improve the calculation efficiency. Finally, the final number of mesh was about 1.35 million. The grid division is shown in Figure 1B (Two vertical sections, 1-1 and 2-2, were selected in the flow path to display the grid division situation).

After conducting a mesh independence test, when the mesh number was above 700,000, the calculated flow rate varied between 1.35 and 1.45 L h^{-1}. With the design emitter flow rate being 1.38 L h^{-1} and considering the calculation time and accuracy, the overall mesh number used was 770,000, which had a calculation error within 5%.

Computing domain was uploaded to Fluent module in ANASYS software, the governing equations were separated by the finite volume method (Li et al., 2019b), and the second-order upwind scheme was used to separate the parameters such as the convection terms. The coupling of velocity and pressure was solved by the algorithm of Semi-Implicit Method for Pressure Linked Equations (SIMPLE) (Feng et al., 2018).

For the simulation of particle movement, three different turbulence models, which were Standard k-ε model, RNG k-ε model and LES (Large Eddy Simulation) model (Feng et al., 2018), were adopted to calculate the continuous phase flow field in the saw-tooth flow path (Feng et al., 2018). All simulated results were also verified by using the test results of hydraulic performance and the DPIV by Liu et al. (2016), and the optimal calculation model was constructed.

According to the methodology described by Feng et al. (2018), for initial conditions, the emitter inlet was set as a pressure inlet with 0.01, 0.03, 0.05, 0.07, 0.09, 0.1, 0.11, 0.13, and 0.15 MPa, and the emitter outlet was set as a pressure outlet with 0 MPa. Except for the inlet and outlet of the calculation domain, all other surfaces between fluid and wall were wall-type boundaries and set to non-slip boundaries. Standard wall functions were used to solve the near-wall flow. The multiphase flow model of standard Euler–Lagrange model was used to simulate particle motion. The sediment density was set to 2500 kg m^{-3}, the volume fraction was 0.03, and the particle size was 100 μm. The flow rate of the outlet and the residual value were used to judge the convergence. When the flow rate of the outlet was basically stable and the residual value was less than 10^{-5}, the iteration was considered to have converged.

After calculating the velocity vector, turbulence intensity of water and particle under different boundary conditions by the simulation model, Tecplot software was used for data post-processing (Feng et al., 2018). Flow index was adopted to analyze the hydraulic performance of each flow path. The discharge data was used to fit the hydraulic characteristic curve under different pressures (0.01, 0.03, 0.05, 0.07, 0.09, 0.10, 0.11, 0.13 and 0.15 MPa), then the effect of flow path structure on the flow index was analyzed. The anti-clogging performance of the different flow paths was also evaluated by using velocity vector and turbulence intensity (Feng et al., 2018).

Results and Discussion

The flow coefficients and flow indexes obtained by the hydraulic performance test and simulated by standard k-ε model, RNG k-ε model and LES model are in Table 2. The hydraulic performance curves of the saw-tooth flow path obtained by the hydraulic performance test according to the requirements of "Technical Specification and Test Method for Irrigators of Agricultural irrigation Equipment" (GB/T17187-1997) and simulated by standard k-ε model, RNG k-ε model and LES model are shown in Figure 2. Compared with the Rated flow rate provided by the manufacturer, the differences calculated by three models at the rated working pressure (0.1 MPa) were 18, 9 and 6%, respectively. These results illustrate that the flow-pressure variation trend of the three models was the same. Among them, the differences calculated by the standard k-ε model were largest and all of them were greater than the measured values. The difference calculated by the LES model was minimum.

In order to comprehensively verify the accuracy of simulation model, the velocity distribution obtained by Liu et al. (2016) was also introduced. The velocity distribution characteristics in the structure unit of saw-tooth flow path obtained by DPIV and simulation are shown in Figure 3.

Figures 3A, B and C show the velocity distribution of the internal flow field obtained by the standard k-ε model, RNG k-ε model and LES model under rated pressure. Figure 3D is the test result of DPIV under rated pressure. The velocity distribution obtained by three simulation models (Figures 3A, B and C) were similar to that of the test result of DPIV (Figure 3D). The velocity near the center of the flow passage was relatively high, which is the main flow area. Near the corner

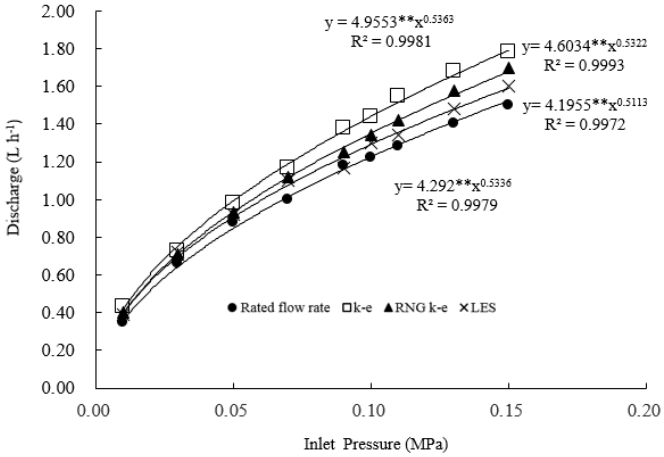

** - Significant at p ≤ 0.05 by F test.

Figure 2. The hydraulic performance curve of different simulation models

Table 2. Flow coefficient (k) and flow index (x) calculated by different models (standard k-ε, RNG k-ε, and LES)

	Standard k-ε model	RNG k-ε model	LES model	Rated flow rate
Flow coefficient k	4.95	4.60	4.20	4.29
Flow index x	0.54	0.53	0.51	0.53

RNG – Re- normalization Group; LES – Large Eddy Simulation

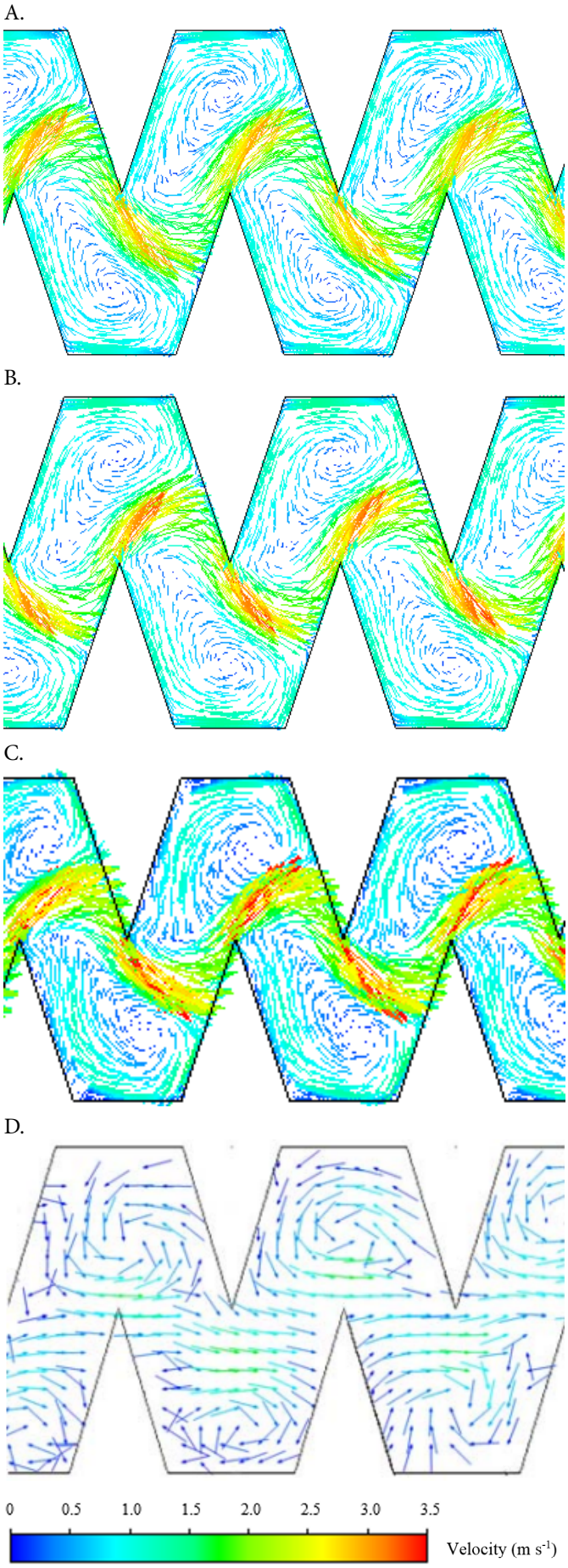

Figure 3. Velocity distribution in structure unit of flow path by Standard k-ε model (A), RNG k-ε model (B), LES model (C) and DPIV model (D)

and tip of the flow path, the velocity was low, which is the non-mainstream area (Areas with relatively less concentrated flow and lower flow velocity). In this area, there was the structure of the vortex. In the mainstream area (Areas with relatively concentrated flow and high flow velocity), the velocity gradient changed obviously compared with that in the non-mainstream area, the turbulence degree was stronger, and the energy dissipation efficiency was high (Li et al., 2015; Liu et al., 2016).

In theory, the main difference between the RNG k-ε model (Figure 3B) and the standard k-ε model (Figure 3A) is the correction of the coefficient in the ε equation. The RNG k-ε model considered the influence of high strain rate or large curvature surface, and the anisotropy effect of turbulence is taken into account to a certain extent, which improves the accuracy of the model in the case of revortex and large curvature (Liu et al., 2016) and is more suitable for the calculation of complex turbulence in the flow path of emitter (Figure 3B). Although LES model has high computational accuracy (Figure 3C), it has high requirements on mesh scale. The mesh must be refined enough to distinguish the turbulent structure. Moreover, LES model (Figure 3C) is an unsteady calculation method, and the calculation is complicated and time-consuming (Liu et al., 2021b; Zhou et al., 2021). Therefore, LES is not the main method for solving the complex turbulent flow field of the emitter.

Considering the calculation accuracy and efficiency, RNG k-ε model was the most suitable for the simulation of the flow field in the emitter.

Hydraulic performance curves of five types of flow paths are shown in Figure 4. The flow indexes were 0.4975 for fractal flow path, 0.4988 for saw-tooth flow path, 0.4995 for trapezoid flow path, 0.5191 for rectangle flow path, and 0.5202 for triangle flow path. For the fractal flow path and saw-tooth flow path, their flow indexes were close to 0.5, which illustrated that their hydraulic performances were relatively optimal.

The flow index represents the flow pattern of water in the emitter and the sensitivity of the flow rate to pressure change (Elbana et al., 2012; Feng et al., 2018). The higher the value, the more sensitive the flow rate to changes in pressure, which explains why the hydraulic performance is low, and vice-versa (Markku et al., 2006; Muhammad et al., 2021). In this paper, the flow indexes of the fractal and saw-tooth flow path were the lowest, which shows that their flow rate was less sensitive to pressure changes. They had better hydraulic performance.

The turbulence intensity distribution of different flow paths is shown in Figure 5. The turbulence intensities in the trapezoid flow path (Figure 5A), triangle flow path (Figure 5B) and rectangle flow path (Figure 5C) were relatively low. They were 0.11-0.56, 0.10-0.50 and 0.11-0.58, respectively. The turbulence intensities in the fractal flow path (Figure 5D) and the saw-tooth flow path (Figure 5E) were relatively high. They were 0.14-0.74 and 0.12-0.69, respectively. There was also no corner region of the polar turbulence intensity. In the trapezoid flow path (Figure 5A), in the tooth tip of triangular flow path (Figure 5B) and in the wall corner of the rectangular flow path (Figure 5C), there were obvious areas of low turbulence intensity.

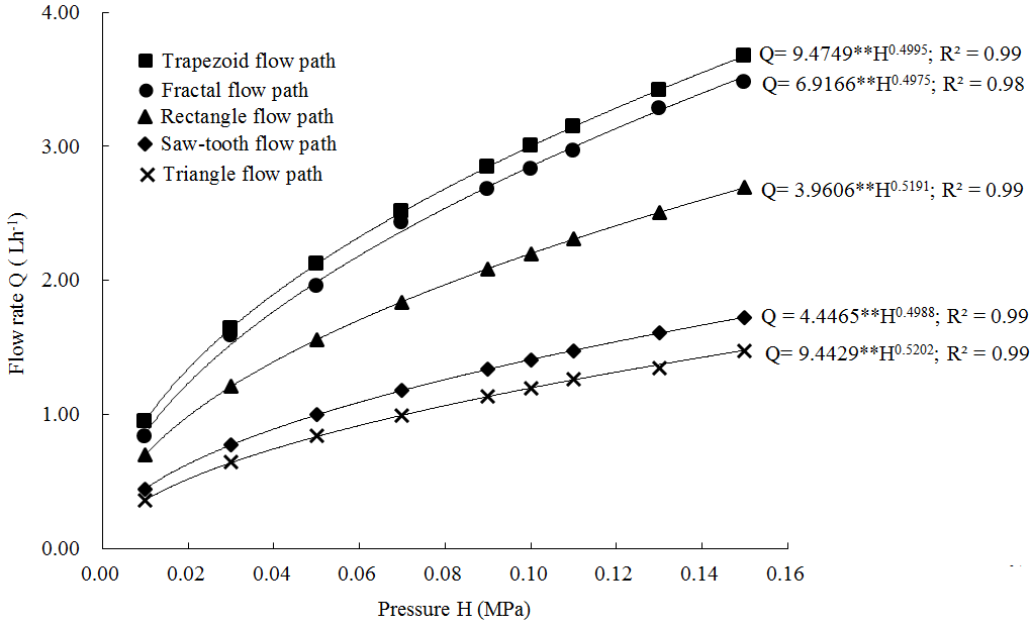

** - Significant at p ≤ 0.05 by F test.

Figure 4. The hydraulic performance curve of different flow paths

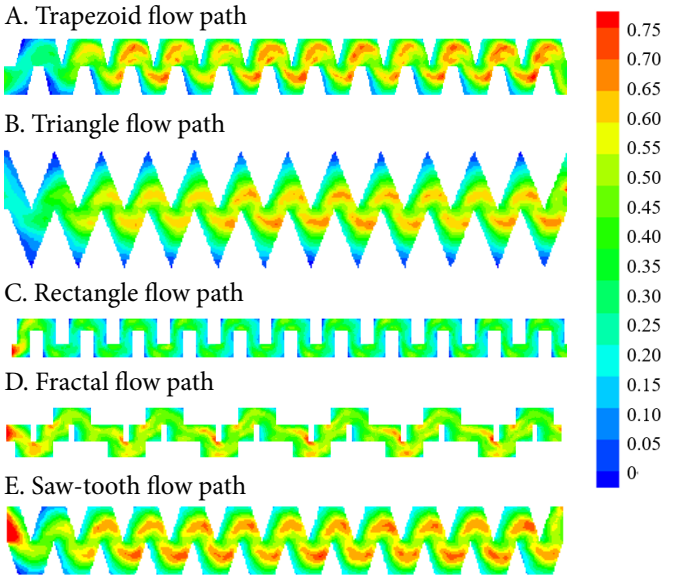

Figure 5. Turbulence intensity in different flow paths

Because areas with low turbulence intensity have lower water flow velocities, their ability to carry sediment is relatively weak (Li et al., 2019b). The sediment is easy to deposit in areas of low turbulence intensity, causing the clogging of the emitter (Li et al., 2012; Song et al., 2020). Through this study, it was found that both the fractal and saw-tooth flow paths do not have areas where turbulence tends to decrease. Therefore, among all flow paths, the anti-clogging performance of fractal and saw-tooth flow paths were relatively high.

The velocity vector distributions for structural units with fractal and saw-tooth flow paths were also analyzed, as shown in Figure 6. There were vortices in the non-mainstream area of fractal flow path (Figure 6A) and saw-tooth flow path (Figure 6B), which can scour the wall surface and is not conducive to the deposition of clogging materials (Li et al., 2019a; Feng et al., 2019). It is worth noting that the velocity in the main stream area of the fractal flow path was the highest,

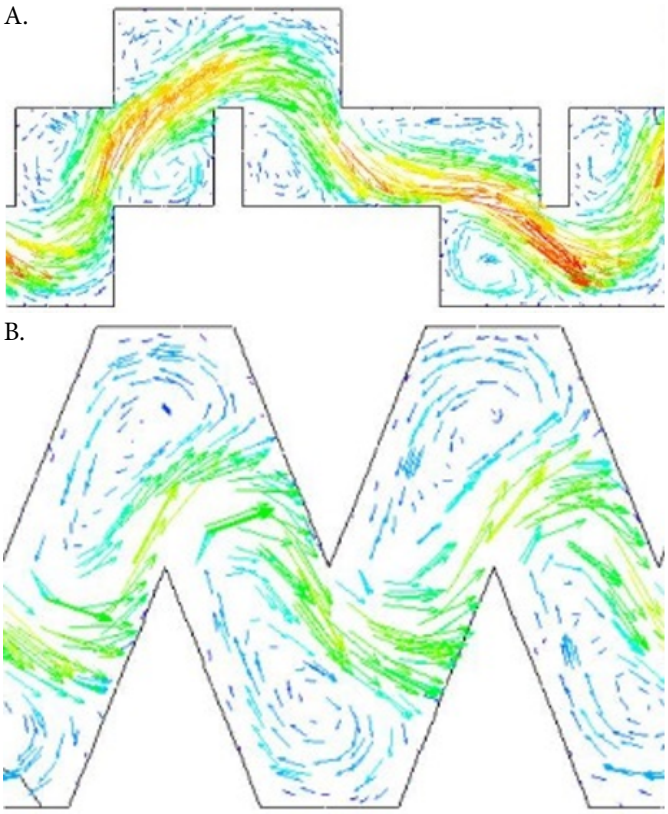

Figure 6. Velocity vector distribution in fractal flow path (A) and saw-tooth flow path (B)

and the velocity near the wall was also the highest (Figure 6A). The higher the flow velocity inside the flow path, the greater the ability to wash away particles, and at the same time, it is easier to carry the washed particles out of the flow path (Han et al., 2018; Jiao et al., 2020; Liu et al., 2021a;). Therefore, based on the analysis of the vector distribution characteristics of turbulence intensity and velocity in different flow path structures, the anti-clogging performance of fractal flow path is relatively optimal.

Conclusions

1. RNG k - ε model was the most suitable to simulate the emitter water movement.

2. The hydraulic performances of fractal flow path and saw-tooth flow path were relatively optimal.

3. The anti-clogging performance of the fractal flow path was relatively optimal.

Contribution of authors: Conceptualization: Ji Feng and Yanzheng Liu; Methodology: Ji Feng, Haisheng Liu and Haosu Sun; Formal analysis and investigation: Ji Feng and Changjian Ma; Writing: original draft preparation: Ji Feng and Haisheng Liu; Writing: Ji Feng and Haisheng Liu; review and editing: Ji Feng and Haisheng Liu; Funding acquisition: Ji Feng, Song Xue and Weinan Wang; Resources: Jiangli Wen; Supervision: Puchen Shi.

Supplementary documents: There is no supplementary research data.

Conflict of Interest: The authors state no conflict of interest, whether financial or otherwise, that may have influenced the preparation or completion of the work.

Acknowledgments: We are grateful for financial support from the R&D Program of Beijing Municipal Educational Commission (KM202312448001), Young Elite Scientists Sponsorship Program by BAST(BYESS2023190) and Beijing Vocational College Excellent Young Key Teacher Cultivation Project (2024090143).

Literature Cited

Chai, H. The use of filters in micro-irrigation systems. Modern Agriculture, v.10, p.55-56, 2016.

Elbana, M.; Cartagena, F. R. D.; Puig-Bargués, J. Effectiveness of sand media filters for removing turbidity and recovering dissolved oxygen from a reclaimed effluent used for micro-irrigation. Agricultural Water Management, v.111, p.27-33, 2012. https://doi.org/10.1016/j.agwat.2012.04.010

Feng, J.; Li, Y.; Liu, Z.; Muhammad, T.; Wu, R. Composite clogging characteristics of emitters in drip irrigation systems. Irrigation Science, v.37, p.105-122, 2019. https://doi.org/10.1007/s00271-018-0605-9

Feng, J.; Li, Y.; Wang, W.; Xue, S. Effect of optimization forms of flow path on emitter hydraulic and anti-clogging performance in drip irrigation system. Irrigation Science, v.36, p.37-47, 2018. https://doi.org/10.1007/s00271-017-0561-9

Han, S.; Li, Y.; Xu, F.; Sun, D.; Feng, J. Effect of lateral flushing on emitter clogging under drip irrigation with yellow river water and a suitable method. Irrigation and Drainage, v.67, p.199-209, 2018. https://doi.org/10.1002/ird.2193

Han, S.; Li, Y.; Zhou, B.; Liu, Z.; Feng, J.; Xiao, Y. An in-situ accelerated experimental testing method for drip irrigation emitter clogging with inferior water. Agricultural Water Management, v.212, p.136-154, 2019. https://doi.org/10.1016/j.agwat.2018.08.024

Jiao, Y.; Feng, J.; Liu, Y.; Yang, L.; Han, M. Sustainable operation mode of a sand filter in a drip irrigation system using Yellow River water in an arid area. Water Science & Technology Water Supply, v.20, p.3636-3645, 2020. https://doi.org/10.2166/ws.2020.217

Li, Y.; Feng, J.; Xue, S.; Muhammad, T.; Chen, X.; W.; Zhou, B. Formation mechanism for emitter composite-clogging in drip irrigation system. Irrigation Science, v.37, p.169-181, 2019a. https://doi.org/10.1007/s00271-018-0612-x

Li, Y.; Liu, Y.; Li, G.; Xu, W.; Liu, S.; Ren, M.; Yan, D.; Yang, P. Surface topographic characteristics of suspended particulates in reclaimed wastewater and effects on clogging in labyrinth drip irrigation emitters. Irrigation Science, v.30, p.43-56, 2012. https://doi.org/10.1007/s00271-010-0257-x

Li, Y.; Song, P.; Pei, Y.; Feng, J. Effects of lateral flushing on emitter clogging and biofilm components in drip irrigation systems with reclaimed water. Irrigation Science, v.33, p.235-245, 2015. https://doi.org/10.1007/s00271-015-0462-8

Li, Y.; Pan, J.; Chen, X.; Xue, S.; Feng, J.; Muhammad, T.; Zhou, B. Dynamic effects of chemical precipitates on drip irrigation system clogging using water with high sediment and salt loads. Agricultural Water Management, v.213, p.833-842, 2019b. https://doi.org/10.1016/j.agwat.2018.11.021

Liu, H.; Sun, H.; Li, Y.; Feng, J.; Song, P.; Zhang, M. Visualizing particle movement in flat drip irrigation emitters with digital particle image velocimetry. Irrigation and Drainage, v.65, p.390-403, 2016. https://doi.org/10.1002/ird.2000

Liu, Z.; Luccio, M.; Garcia, S.; Puig-Bargues, J.; Zhao, X.; Trueba, A.; Muhammad, T.; Xiao, Y.; Li, Y. Effect of magnetic field on calcium - silica fouling and interactions in brackish water distribution systems. Science of the Total Environment, v.798, e148900, 2021a. https://doi.org/10.1016/j.scitotenv.2021.148900

Liu, Z.; Muhammad, T.; Puig-Bargués, J.; Han, S.; Ma, Y.; Li, Y. Horizontal roughing filter for reducing emitter composite clogging in drip irrigation systems using high sediment water. Agricultural Water Management, v.258, e107215, 2021b. https://doi.org/10.1016/j.agwat.2021.107215

Markku, J. L.; Laxander, M.; Miettinen, I. T.; Hirvonen, A.; Vartiainen, T.; Martikainen, P. J. The effects of changing water flow velocity on the formation of biofilms and water quality in pilot distribution system consisting of copper or polyethylene pipes. Water Research, v.40, p.2151-2160, 2006. https://doi.org/10.1016/j.watres.2006.04.010

Muhammad, T.; Zhou, B.; Liu, Z.; Chen, X.; Li, Y. Effects of phosphorus-fertigation on emitter clogging in drip irrigation system with saline water. Agricultural Water Management, v.243, e106392, 2021. https://doi.org/10.1016/j.agwat.2020.106392

Nakayama, F. S.; Bucks, D. A. Water quality in drip/trickle irrigation: a review. Irrigation Science, v.12, p.187-192, 1991.

Song, P.; Xiao, Y.; Ren, Z.; Brooks, J. P.; Li, Y. Electrochemical biofilm control by reconstructing microbial community in agricultural water distribution systems. Journal of Hazardous Materials, v.403, e123616, 2020. https://doi.org/10.1016/j.jhazmat.2020.123616

Tayel, M. Y.; Pibars, S. K.; Mansour, H. A. G. Effect of drip irrigation method, nitrogen source, and flushing schedule on emitter clogging. Agricultural Sciences, v.4, p.131-137, 2013. https://doi.org/10.4236/as.2013.43020

Xue, S. Emitter clogging material formation mechanism and growth kinetics model in drip irrigation system. China Agricultural University, Beijing, 2016. 56p.

Zhou, B.; Hou, P.; Xiao, Y.; Song, P.; Li, Y. Visualizing, quantifying, and controlling local hydrodynamic effects on biofilm accumulation in complex flow paths. Journal of Hazardous Materials, v.416, e125937, 2021. https://doi.org/10.1016/j.jhazmat.2021.125937